Coherent Coupling of Excitons and Trions in a Photoexcited CdTe/CdMgTe Quantum Well

G. Moody,[1,2] I. A. Akimov,[3,4] H. Li,[1] R. Singh,[1,2] D. R. Yakovlev,[3,4] G. Karczewski,[5] M. Wiater,[5] T. Wojtowicz,[5] M. Bayer,[3] and S. T. Cundiff[1,2,*]

[1]*JILA, University of Colorado & National Institute of Standards and Technology, Boulder, Colorado 80309-0440, USA*
[2]*Department of Physics, University of Colorado, Boulder, Colorado 80309-0390, USA*
[3]*Experimentelle Physik 2, Technische Universität Dortmund, D-44221 Dortmund, Germany*
[4]*A. F. Ioffe Physical-Technical Institute, Russian Academy of Sciences, 194021 St. Petersburg, Russia*
[5]*Institute of Physics, Polish Academy of Sciences, PL-02668 Warsaw, Poland*
(Received 30 July 2013; published 3 March 2014)

We present zero-, one-, and two-quantum two-dimensional coherent spectra of excitons and trions in a CdTe/(Cd,Mg)Te quantum well. The set of spectra provides a unique and comprehensive picture of the coherent nonlinear optical response. Distinct peaks in the spectra are manifestations of exciton-exciton and exciton-trion coherent coupling. Excellent agreement using density matrix calculations highlights the essential role of many-body effects on the coupling. Strong exciton-trion coherent interactions open up the possibility for novel conditional control schemes in coherent optoelectronics.

Coherent phenomena in semiconductor nanostructures have garnered considerable interest in recent years for potential applications in spintronics [1], quantum optics, and quantum information processing [2]. Among various ensemble spin systems, a two-dimensional electron gas (2DEG) in a modulation-doped quantum well is particularly interesting because a dense spin ensemble exhibiting little to no inhomogeneity is readily grown using epitaxial methods. At low temperature, the band-edge optical properties of a modulation-doped quantum well are dominated by Coulomb-bound electron-hole pairs (excitons) and charged excitons (trions) [3,4], analogous to H and H^- or H_2^+ in atomic physics, respectively.

Exciton and trion resonances have been exploited for a variety of coherent phenomena, including long-lived spin oscillations [5,6], coherent spin rotations about the Bloch sphere [7], quantum memories [8], electromagnetically induced transparency (EIT) [9], and coherent control of quantum Hall systems [10]. These processes rely on manipulation of the 2DEG through coherent light-matter interactions of the exciton and trion transitions, whose optical properties are influenced by many-body effects (MBEs) inherent to semiconductors. For example, the fidelity of collective electron spin rotations is hindered by exciton-trion interactions, and excitation of the exciton can reduce the polarized 2DEG spin coherence time by an order of magnitude [7]. Additionally, Coulomb interactions can limit the level of achievable transparency in EIT experiments to a few percent [9]. In a quantum Hall system, Coulomb correlations play a crucial role in the transient optical properties and coupling between Landau levels [11].

These examples illustrate the impact of MBEs on the coherent response of a 2DEG, which have not been adequately characterized. Moreover, coherent coupling between excitons and trions is interesting, since it requires the complexes to be in close proximity to be significant. Typically, trions are localized at cryogenic temperatures, while excitons can be spatially more extended [12]. The effective spatial overlap of the wave functions determines their coupling strength. Exciton-trion interactions have so far been regarded as incoherent and therefore detrimental, e.g., leading to enhanced dephasing. Conversely, coherent exciton-trion coupling, which has not been previously demonstrated, could lead to a paradigm shift in the understanding of the optical properties of 2DEGs, since it might be exploited for conditional operations in coherent optoelectronics. Thus, the development of novel devices requires establishing the influence of MBEs on the nonlinear optical properties of 2DEGs.

Linear spectroscopies provide some insight in this regard, revealing three-particle interactions that govern trion formation [13,14] and oscillator-strength-stealing phenomena [15,16]. Nonlinear spectroscopies such as transient absorption and four-wave mixing (FWM) techniques are sensitive to interactions mediated through Coulomb forces [17] or local fields [18]. These techniques have been used to probe for signatures of exciton-trion correlations stemming from phase-space filling and fermionic exchange [19,20]; however, MBEs such as excitation-induced dephasing (EID) [21] and excitation-induced energy shift (EIS) [22] cannot be reliably distinguished using one-dimensional techniques since the numerous quantum pathways contributing to the nonlinear optical response are not sufficiently separated [22,23].

In this Letter, we use optical two-dimensional coherent spectroscopy (2DCS) [24]—an enhanced version of three-pulse transient FWM—to overcome these limitations, thus providing unique insight into MBEs of optically

excited carriers in a 2DEG. We present a set of 2D spectra from a nominally undoped CdTe/(Cd,Mg)Te QW, which has not been previously studied using 2DCS. Specific quantum pathways are isolated by the different types of 2D spectra, enabling differentiation between many-body contributions to the coherent nonlinear optical response [25]. Each type of spectrum better separates the quantum pathways associated with interactions in the system compared to its one-dimensional counterparts; however, we demonstrate that only when the collection of different types of 2D spectra are considered can a comprehensive picture of the nonlinear optical response be established. Excellent agreement between density matrix calculations and the measurements reveals the essential role of MBEs on coherent excitonic interactions in the QW.

The sample consists of a single 20 nm wide CdTe/CdMgTe QW grown by molecular beam epitaxy on a (100)-oriented GaAs substrate. The QW is separated from the substrate by a CdTe/CdMgTe superlattice grown on a thick CdMgTe buffer layer and is isolated from the surface by a 100 nm CdMgTe barrier. The sample is nominally undoped, but due to residual impurities and charge redistribution to surface states, the QW at low temperature contains a dilute 2DEG (verified through magneto-photoluminescence spectra, data not shown). The sample is mounted on a sapphire disk and the substrate is chemically removed for transmission experiments. In the absence of MBEs, the exciton and trion can be considered two independent two-level systems as shown in Fig. 1(a) and reported in Ref. [19]. Optical excitation generates excitons and trions with total angular momentum projections along the growth direction of $J_X = \pm 1$ and $J_{T^-} = \pm 3/2$, respectively. The optically active transitions accessible using circularly polarized light ($\sigma+$) are shown in Fig. 1(a) for the exciton, comprised of a spin $J_e = -1/2$ electron (thin arrow) and spin $J_h = +3/2$ heavy hole (thick arrow), and for the negative trion, consisting of two opposite spin electrons in a singlet state correlated with a spin $J_h = +3/2$ heavy hole.

2DCS experiments are performed using four phase-stabilized pulses propagating in the box geometry [26]. The pulses, obtained from a mode-locked laser operating at a 76 MHz repetition rate, have a ~150 fs duration and are cocircularly polarized. Three of the pulses A, B, and C with wave vectors $\mathbf{k}_A$, $\mathbf{k}_B$, and $\mathbf{k}_C$, respectively, are focused to a single ~50 μm spot on the sample, which is kept at a temperature of 6 K. The exciton and trion excitation densities are kept below ~5×10^9 cm^{-2} to remain in the $\chi^{(3)}$ regime. The pulses generate a FWM signal that is detected along the phase-matched direction $\mathbf{k}_s = -\mathbf{k}_A + \mathbf{k}_B + \mathbf{k}_C$, which necessarily requires that pulse A acts as a conjugate pulse irrespective of pulse time ordering, as shown in the schematic diagram in Fig. 1(c). The signal is heterodyned with a phase-stabilized reference pulse and their interference is spectrally resolved with 20 μeV resolution. For a rephasing experiment,
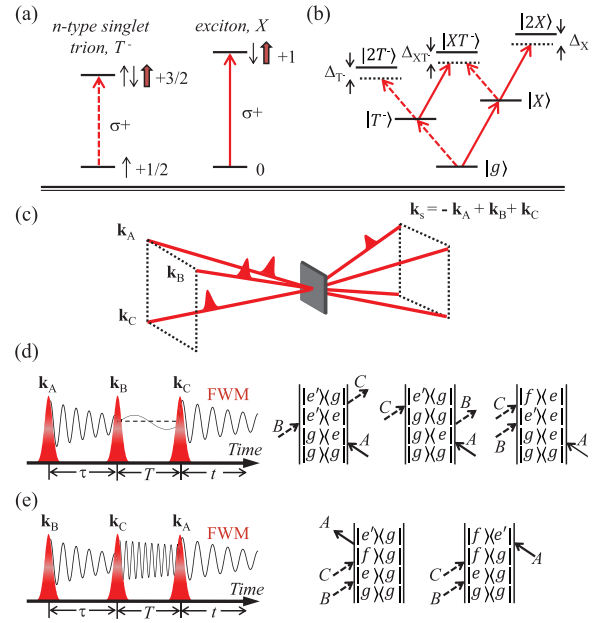

FIG. 1 (color online). (a) Exciton and negative trion optical transitions accessible using circularly polarized light ($\sigma+$). (b) The exciton and trion nonlinear response is modeled using a six-level energy scheme consisting of a ground state ($|g\rangle$), singly excited exciton ($|X\rangle$) and trion ($|T^-\rangle$) states, doubly excited exciton ($|2X\rangle$) and trion ($|2T^-\rangle$) states with an energy shift Δ_X and Δ_{T^-}, respectively, and a doubly excited mixed exciton-trion state ($|XT^-\rangle$) shifted from the exciton + trion energy by Δ_{XT^-}. (c) Geometry of the incident beams and the FWM signal. The pulse time ordering and generalized double-sided Feynman diagrams are shown for the (d) rephasing zero- and one-quantum and (e) two-quantum sequences.

interferograms are measured while the delay τ between the first two pulses incident on the sample, A and B, is scanned with interferometric precision, as shown in the timing sequence in Fig. 1(d). The FWM signal is Fourier transformed with respect to τ to generate a rephasing one-quantum spectrum that correlates the excitation and emission energies for a fixed delay $T = 200$ fs. A rephasing zero-quantum spectrum, which is sensitive to population dynamics and nonradiative coherent superpositions between states [27,28], is acquired by scanning and Fourier transforming the signal with respect to T, the delay between pulses B and C. Alternatively, the pulse time ordering can be adjusted so that pulse A is incident on the sample last, as depicted in the timing sequence in Fig. 1(e). The delay T between pulses C and A is scanned, and the signal is Fourier transformed with respect to T to generate a two-quantum spectrum correlating the two-quantum energies with the one-quantum emission energies.

The absolute value of the rephasing one-quantum spectrum is shown in Fig. 2(a). The vertical axis is plotted as negative excitation photon energy since the coherences oscillate at negative frequencies during τ with respect to the coherences during t. The spectrum features two peaks on the diagonal line corresponding to excitation and emission
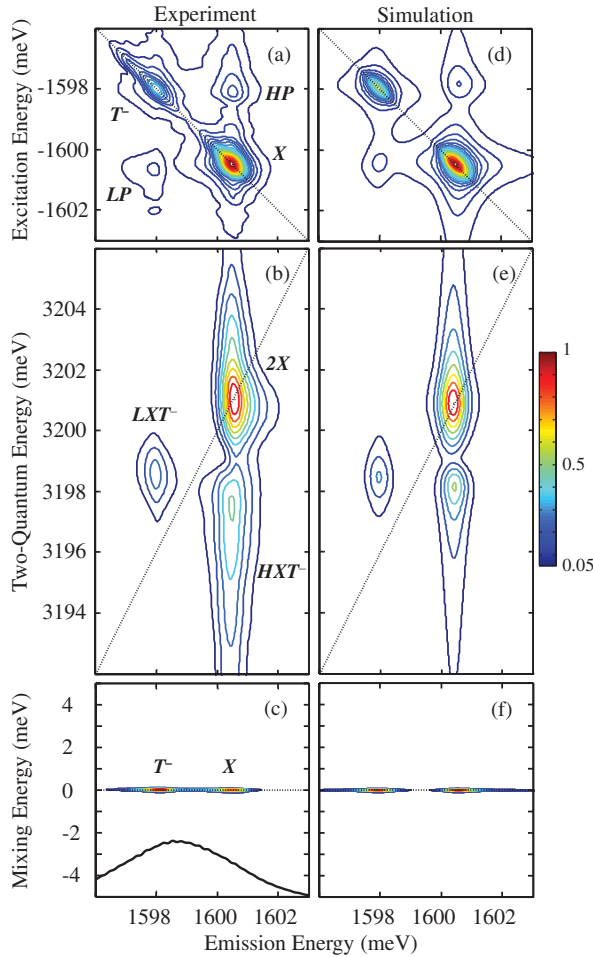
FIG. 2 (color online). Normalized experimental rephasing (a) one-quantum spectrum of the exciton (X), trion (T^-), and their interaction (LP and HP). Two-quantum coherences of the exciton ($2X$) and the mixed exciton-trion state (LXT^- and HXT^-) appear in the experimental two-quantum spectrum shown in (b). X and T^- population peaks appear in the zero-quantum spectrum in (c). The excitation laser spectrum for all experiments is shown in the inset to (c). Panels (d)–(f) are the corresponding simulated spectra. The color bar indicates the normalized amplitude of each spectrum.

at the exciton (X) and trion (T^-) transitions. The cross-diagonal and diagonal slices of each peak are simultaneously fit to analytical functions to determine the full width at half maximum of the homogeneous and inhomogeneous linewidths [29]. For the exciton, the homogeneous linewidth is ≈ 0.15 meV, which is larger, but a similar order of magnitude, compared to excitons in GaAs QWs for a similar excitation density [30,31]. The trion homogeneous linewidth is ≈ 0.1 meV, and both the exciton and trion resonances are inhomogeneously broadened by ≈ 0.5 meV. The trion resonance is redshifted from the exciton by a 2.7 meV binding energy. This energy is comparable to the biexciton binding energy in In(Ga)As quantum dots, which have been the primary semiconductor system for demonstrating entangled photon pair generation and other nonlinearities such as photon blockade [32]. Although the

exciton and trion can be considered two independent systems, the appearance of low (LP) and high (HP) emission energy cross peaks in Fig. 2(a) reveals that the exciton and trion are quantum mechanically coupled through many-body interactions, since these peaks indicate excitation at one energy and emission at the other. This coupling is to be distinguished from polarization interference between two independent systems, which would not lead to LP and HP.

To establish the origin of LP and HP, we probe for coherent coupling mechanisms by acquiring a two-quantum spectrum, shown in Fig. 2(b), for which a nonzero signal arises only if coherent many-body interactions between resonances exist [33–36]. The spectrum features two cross peaks (LXT^- and HXT^-) attributed to a collective exciton-trion two-quantum coherence and their appearance necessarily implies that the exciton and trion interact coherently. The peak ($2X$) on the diagonal line arises from coherent interactions between two excitons in the QW. The absence of a two-trion peak, which would appear on the diagonal line at a two-quantum energy equal to twice the trion energy, indicates that coherent coupling between trions is absent due to spatial separation. Coherent coupling between resonances is often accompanied by peaks associated with nonradiative Raman-like coherences between transitions in a rephasing zero-quantum spectrum [35], which is shown in Fig. 2(c). The spectrum features two peaks at zero mixing energy and at the trion (T^-) and exciton (X) emission energies, corresponding to the system being in a ground or excited state population during the delay T. Simulations discussed later demonstrate that Raman-like cross peaks at ± 2.7 meV mixing energy are too weak to appear because MBEs enhance X and T^-.

To quantify the strength of the exciton-trion coupling, we follow a similar approach as Kasprzak *et al.* and define the relative coupling strength (RCS) as the ratio of HP to the geometrical average of X and T^- in Fig. 2(a), which takes into account differences in oscillator strengths and spatial and spectral overlap of the excitation pulses with the resonances [37]. The exciton-trion RCS measured here is ≈ 0.33, which is similar to an RCS of $\lesssim 0.4$ measured for the majority of excitons in semiconductor quantum dots [37]. The similar RCS observed here suggests that many-body interactions giving rise to coherent coupling between excitons and trions have a similar impact on coherent optoelectronic applications as for excitons in quantum dots.

The collection of 2D spectra provides a unique perspective into the coherent nonlinear optical response of excitons, trions, and a 2DEG. To better understand the effects of exciton-trion interactions, we simulate the spectra by analytically solving a perturbative expansion of the density matrix for a six-level system, shown in Fig. 1(b). The energy scheme consists of a ground state ($|g\rangle$), singly excited exciton ($|X\rangle$) and trion ($|T^-\rangle$) states, doubly excited states representing exciton-exciton ($|2X\rangle$) and trion-trion ($|2T^-\rangle$) correlations, and a doubly excited mixed exciton-trion state ($|XT^-\rangle$). In the absence of MBEs, such a level diagram is equivalent through a Hilbert space transformation [38] to

four independent two-level systems, for which no signals associated with coupling are expected. In this case, for the six-level energy diagram, quantum pathways involving the doubly excited states cancel pathways associated with interactions between the singly excited states so that spectral signatures of coupling are absent. Incomplete cancellation of the interaction pathways, and therefore exciton-exciton, trion-trion, and exciton-trion MBEs, is modeled by breaking the equivalence of the lower and upper transitions, as was suggested in Ref. [39] and previously applied to model exciton-exciton interactions in quantum dots [37,40]. EID and EIS are modeled by altering the dephasing rate and transition energy, respectively, of the upper transitions compared to the lower transitions.

Quantum pathways contributing to the nonlinear optical response are characterized by the Feynman diagrams in Figs. 1(d) and 1(e), written in a generalized form for which the states labeled with $|e\rangle$ and $|e'\rangle$ can be replaced with $|X\rangle$ or $|T^-\rangle$, and the state labeled by $|f\rangle$ with $|2X\rangle$, $|2T^-\rangle$, or $|XT^-\rangle$. Expanding the diagrams in Fig. 1(d) results in 14 pathways that contribute to the rephasing zero- and one-quantum spectra. Similarly, for the two-quantum spectrum, the diagrams in Fig. 1(e) can be expanded into 12 pathways. Perturbation calculations are performed using Dirac delta function pulses in time. Inhomogeneity that allows for uncorrelated broadening between transitions is included by integrating the third-order polarization over a Gaussian distribution of transition frequencies [41]. The homogeneous and inhomogeneous linewidths are adjusted to match the measurements. The coefficient characterizing the level of correlation between transition energy fluctuations R is set equal to zero for all pathways that involve both the exciton and trion transitions; otherwise it is set equal to unity. The model cannot account for finite bandwidth effects of the excitation pulses on the measurements. Nonetheless, the amplitudes are matched by setting the optical dipole moment of the trion transition equal to 80% of the exciton transition for all simulated spectra.

Simulated spectra are shown in the right column of Fig. 2. The measurements are reproduced for one specific set of parameters for all spectra. We would like to stress this point: the complete collection of 2D measurements is necessary to provide enough constraints to identify the type of couplings in the system. Without sufficient separation of the quantum pathways, either by analyzing a subset of the spectra or probing the sample using one-dimensional methods, a comprehensive picture of the coherent nonlinear optical response cannot be established. The simulations demonstrate that the inclusion of MBEs is essential to model the experimental data. Without them, coupling peaks LP and HP would be absent and the two-quantum signal would be zero.

Comparison between experiment and simulations reveals that the cross peaks in both the one- and two-quantum spectra originate from an EIS of the mixed $|XT^-\rangle$ state equal to $\Delta_{XT^-} \approx \pm 50~\mu$eV. Similarly, the $2X$ peak in Fig. 2(b) stems from an EIS equal to $\Delta_X \approx \pm 0.12$ meV. The two-quantum coherence linewidths are reproduced by

setting the $|g\rangle \to |2X\rangle$ and $|g\rangle \to |XT^-\rangle$ dephasing rates equal to 0.3 and 0.2 meV, respectively, indicating that the correlated states dephase in a picosecond time scale. Absence of a trion two-quantum peak ($2T^-$) is modeled by maintaining the equivalence of the $|T^-\rangle \to |2T^-\rangle$ and $|g\rangle \to |T^-\rangle$ transitions. The unequal strength of the LXT^- and HXT^- peaks in the two-quantum spectrum originates from the EID of the exciton transition in the presence of the trion, which is modeled by increasing the dephasing rate of the $|T^-\rangle \to |XT^-\rangle$ transition compared to the $|g\rangle \to |X\rangle$ transition. Through EID, the HXT^- peak destructively interferes with the $2X$ peak at the exciton + trion energy. The same EID mechanism enhances HP compared to LP in Fig. 2(a), and the symmetric shape of these peaks is reproduced only when $R = 0$ for the quantum pathways involving both the exciton and trion, indicating that fluctuations of their respective transition energies are uncorrelated. In Fig. 2(a), MBEs also enhance the exciton peak relative to the trion peak, which is weaker due the absence of interactions between trions. The simulation demonstrates that the nonradiative Raman-like coherences in the zero-quantum spectrum are concealed by many-body effects.

In summary, coherent interactions between excitons and trions in a CdTe/CdMgTe QW have been studied using optical 2DCS. The collection of zero-, one-, and two-quantum spectra provides sufficient constraints for establishing how MBEs influence the coherent optical response of excitons, trions and a 2DEG in a QW. Excellent agreement between density matrix calculations and the experiment is obtained, from which several conclusions can be drawn. First, cross peaks in the spectra appear from an excitation-induced energy shift of the mixed exciton-trion state. Second, an asymmetry in the coupling peak amplitudes indicates that the presence of trions enhances the exciton dephasing rate. Third, the shape of the cross peaks in the rephasing one-quantum spectrum indicates that fluctuations in the exciton and trion transition frequencies are uncorrelated. Fourth, a two-quantum coherence signal at the collective exciton + trion energy reveals that the interactions are coherent in nature. Last, the absence of a trion two-quantum signal reveals that trions do not coherently interact due to their spatial separation. These observations cannot be attributed simply to mixing of the exciton and trion wave functions mediated by the 2DEG [42], which has been a useful concept for explaining renormalization of the exciton and trion energies and oscillator-strength-stealing phenomena; instead, the results presented here necessarily require non-linearities arising from coherent exciton-trion interaction effects contributing to the nonlinear response. Optical 2DCS provides a unique perspective into the many-body effects stemming from coherent exciton-trion coupling, which we anticipate will motivate continued theoretical work based on microscopic multiparticle interactions that fully capture the many-body effects between neutral and charged particles residing in a plasma.

---

*cundiff@jila.colorado.edu

[1] *Semiconductor Spintronics and Quantum Computation*, edited by D. D. Awschalom, D. Loss, and N. Samarth (Springer-Verlag, Berlin, 2002).

[2] D. D. Awschalom, L. C. Bassett, A. S. Dzurak, E. L. Hu, and J. R. Petta, Science **339**, 1174 (2013).

[3] M. A. Lampert, Phys. Rev. Lett. **1**, 450 (1958).

[4] K. Kheng, R. T. Cox, Y. Merle d'Aubigné, F. Bassani, K. Saminadayar, and S. Tatarenko, Phys. Rev. Lett. **71**, 1752 (1993).

[5] Z. Chen, R. Bratschitsch, S. G. Carter, S. T. Cundiff, D. R. Yakovlev, G. Karczewski, T. Wojtowicz, and J. Kossut, Phys. Rev. B **75**, 115320 (2007).

[6] E. A. Zhukov, D. R. Yakovlev, M. Gerbracht, G. V. Mikhailov, G. Karczewski, T. Wojtowicz, J. Kossut, and M. Bayer, Phys. Rev. B **79**, 155318 (2009).

[7] C. Phelps, T. Sweeney, R. T. Cox, and H. Wang, Phys. Rev. Lett. **102**, 237402 (2009).

[8] L. Langer, S. V. Poltavtsev, I. A. Yugova, D. R. Yakovlev, G. Karczewski, T. Wojtowicz, J. Kossut, I. A. Akimov, and M. Bayer, Phys. Rev. Lett. **109**, 157403 (2012).

[9] H. Wang and S. O'Leary, J. Opt. Soc. Am. B **29**, A6 (2012).

[10] K. M. Dani, J. Tignon, M. Breit, D. S. Chemla, E. G. Kavousanaki, and I. E. Perakis, Phys. Rev. Lett. **97**, 057401 (2006).

[11] K. M. Dani, E. G. Kavousanaki, J. Tignon, D. S. Chemla, and I. E. Perakis, Solid State Commun. **140**, 72 (2006).

[12] G. V. Astakhov, V. P. Kochereshko, D. R. Yakovlev, W. Ossau, J. Nürnberger, W. Faschinger, G. Landwehr, T. Wojtowicz, G. Karczewski, and J. Kossut, Phys. Rev. B **65**, 115310 (2002).

[13] M. Combescot, J. Tribollet, G. Karczewski, F. Bernardot, C. Testelin, and M. Chamarro, Europhys. Lett. **71**, 431 (2005).

[14] M. T. Portella-Oberli, J. Berney, L. Kappei, F. Morier-Genoud, J. Szczytko, and B. Deveaud-Plédran, Phys. Rev. Lett. **102**, 096402 (2009).

[15] D. Brinkmann, J. Kudrna, P. Gilliot, B. Hönerlage, A. Arnoult, J. Cibert, and S. Tatarenko, Phys. Rev. B **60**, 4474 (1999).

[16] P. Plochocka, P. Kossacki, W. Maślana, J. Cibert, S. Tatarenko, C. Radzewicz, and J. A. Gaj, Phys. Rev. Lett. **92**, 177402 (2004).

[17] T. Meier, P. Thomas, and S. Koch, *Coherent Semiconductor Optics* (Springer-Verlag, Berlin, 2007).

[18] K. Leo, M. Wegener, J. Shah, D. S. Chemla, E. O. Gobel, T. C. Damen, S. Schmitt-Rink, and W. Schäfer, Phys. Rev. Lett. **65**, 1340 (1990).

[19] H. P. Wagner, H.-P. Tranitz, and R. Schuster, Phys. Rev. B **60**, 15542 (1999).

[20] M. T. Portella-Oberli, V. Ciulin, J. H. Berney, B. Deveaud, M. Kutrowski, and T. Wojtowicz, Phys. Rev. B **69**, 235311 (2004).

[21] H. Wang, K. Ferrio, D. G. Steel, Y. Z. Hu, R. Binder, and S. W. Koch, Phys. Rev. Lett. **71**, 1261 (1993).

[22] J. M. Shacklette and S. T. Cundiff, Phys. Rev. B **66**, 045309 (2002).

[23] S. Mukamel, Annu. Rev. Phys. Chem. **51**, 691 (2000).

[24] S. T. Cundiff, A. D. Bristow, M. Siemens, H. Li, G. Moody, D. Karaiskaj, X. Dai, and T. Zhang, IEEE J. Sel. Top. Quantum Electron. **18**, 318 (2012).

[25] X. Li, T. Zhang, C. N. Borca, and S. T. Cundiff, Phys. Rev. Lett. **96**, 057406 (2006).

[26] A. D. Bristow, D. Karaiskaj, X. Dai, T. Zhang, C. Carlsson, K. R. Hagen, R. Jimenez, and S. T. Cundiff, Rev. Sci. Instrum. **80**, 073108 (2009).

[27] X. Dai, A. D. Bristow, D. Karaiskaj, and S. T. Cundiff, Phys. Rev. A **82**, 052503 (2010).

[28] G. Moody, R. Singh, H. Li, I. A. Akimov, M. Bayer, D. Reuter, A. D. Wieck, and S. T. Cundiff, Solid State Commun. **163**, 65 (2013).

[29] M. E. Siemens, G. Moody, H. Li, A. D. Bristow, and S. T. Cundiff, Opt. Express **18**, 17699 (2010).

[30] A. D. Bristow, T. Zhang, M. E. Siemens, S. T. Cundiff, and R. P. Mirin, J. Phys. Chem. B **115**, 5365 (2011).

[31] R. Singh, T. M. Autry, G. Nardin, G. Moody, H. Li, K. Pierz, M. Bieler, and S. T. Cundiff, Phys. Rev. B **88**, 045304 (2013).

[32] R. M. Stevenson, R. J. Young, P. Atkinson, K. Cooper, D. A. Ritchie, and A. J. Shields, Nature (London) **439**, 179 (2006).

[33] X. Dai, M. Richter, H. Li, A. D. Bristow, C. Falvo, S. Mukamel, and S. T. Cundiff, Phys. Rev. Lett. **108**, 193201 (2012).

[34] D. Karaiskaj, A. D. Bristow, L. Yang, X. Dai, R. P. Mirin, S. Mukamel, and S. T. Cundiff, Phys. Rev. Lett. **104**, 117401 (2010).

[35] L. Yang and S. Mukamel, Phys. Rev. Lett. **100**, 057402 (2008).

[36] K. W. Stone, K. Gundogdu, D. B. Turner, X. Li, S. T. Cundiff, and K. A. Nelson, Science **324**, 1169 (2009).

[37] J. Kasprzak, B. Patton, V. Savona, and W. Langbein, Nat. Photonics **5**, 57 (2011).

[38] See Supplemental Material at http://link.aps.org/supplemental/10.1103/PhysRevLett.112.097401 for more details of the energy level scheme and parameters used for the simulation.

[39] K. Bott, O. Heller, D. Bennhardt, S. T. Cundiff, P. Thomas, E. J. Mayer, G. O. Smith, R. Eccleston, J. Kuhl, and K. Ploog, Phys. Rev. B **48**, 17418 (1993).

[40] G. Moody, R. Singh, H. Li, I. A. Akimov, M. Bayer, D. Reuter, A. D. Wieck, A. S. Bracker, D. Gammon, and S. T. Cundiff, Phys. Rev. B **87**, 041304 (2013).

[41] S. T. Cundiff, Phys. Rev. A **49**, 3114 (1994).

[42] R. A. Suris, V. P. Kochereshko, G. V. Astakhov, D. R. Yakovlev, W. Ossau, J. Nürnberger, W. Fashinger, G. Landwehr, T. Wojtowicz, G. Karczewski, and J. Kossut, Phys. Status Solidi B **227**, 343 (2001).